$H_{40}Fe_3O_7P_4$ (816.1): C, 45.62; H, 4.94. Found: C, 45.52; H, 4.99.

The ^{31}P NMR spectrum of the bis-phosphine VI at −64 °C is consistent with the presence of two isomers VIa and VIc (analogous to IIIa and IIIc for the phosphite analogues, vide supra) in a 30:70 ratio. Although the line shape of VIa is unaffected by temperature variations, the signals of VIc are broadened at room temperature, and coalescence is observed at 53 °C in C_6D_6. There was no evidence for isomer VIb (corresponding to IIIb) at −64 °C. This coupled with the higher temperatures required for the interconversion of VIc with VIb suggests that the (axial, axial) conformation of basal phosphines in conformation VIb is disfavored relative to the (axial, equatorial) conformation in VIc. Nonbonded steric interactions, which are expected to be more severe with triethylphosphine relative to trimethyl phosphite,[61] are presumably responsible for the difference between IIIa and VIa, since the axial position is favored in the mono-substituted triiron clusters.[20,28]

Preparation of ESR Samples. Solutions of the anion radicals were prepared at room temperature under an argon atmosphere. They were transferred with the aid of a hypodermic syringe into ESR tubes, which were subsequently sealed under vacuum. For the description of the ESR technique, see ref 62.

Kinetic Measurements. In a bulk electrolysis cell, the solvent, electrolyte, and ligand were placed to obtain a total volume of 27 mL. This solution was prereduced at a potential of −2.0 V. Then 100 mg (0.157 mmol) of $Fe_3(CO)_9(PPh)_2$ was added. The CV of this solution was taken, and the peak current of the first reduction wave of $Fe_3(CO)_9(PPh)_2$ was used as a reference for the initial concentration of the parent cluster. In the constant current mode (2.529 mA), the solution was reduced for 10 min at a potential of −0.8 V corresponding to a reduction of 10% of $Fe_3(CO)_9(PPh)_2$. After electrolysis, the substitution reaction was followed by cyclic voltammetry taken at intervals varying between 2 and 5 min, until the starting material was consumed. The actual concentrations of unreacted starting material were calculated by direct comparison of the peak current of the first reduction wave of $Fe_3(CO)_9(PPh)_2$. Ligand substitutions of the parent cluster were mostly completed within 30–70 min after electrolysis. The solvent and electrolyte consisted of either tetrahydrofuran containing 0.3 M TBAP or acetonitrile containing 0.1 M TBAP. Varying amounts of ligand were added in measured amounts with the aid of a hypodermic syringe.

(61) Cone angle of PEt_3 = 132°, $P(OMe)_3$ = 107°. See: Tolman, C. A. *Chem. Rev.* **1977**, *77*, 313.
(62) Lau, W.; Huffman, J. C.; Kochi, J. K. *Organometallics* **1982**, *1*, 155.

Acknowledgment. We thank J. D. Korp for the crystal structure of IV, M. R. Richmond for helpful discussions, and the National Science Foundation and Robert A. Welch Foundation for financial support. H. H. Ohst is a recipient of a NATO grant administered under the auspices of the German Academic Exchange Service.

Registry No. I, 38903-71-8; $I^{-\cdot}$, 101198-33-8; $I'^{-\cdot}$, 101011-28-3; $II^{-\cdot}$, 39040-36-3; $II'^{-\cdot}$, 101011-23-8; IIa, 101011-13-6; IIb, 101011-14-7; IIIa, 101011-15-8; IIIb, 101011-16-9; IIIc, 101141-53-1; IVa, 101011-17-0; IVb, 101141-54-2; $V^{-\cdot}$, 101011-27-2; $V'^{-\cdot}$, 101011-25-0; Va, 101011-18-1; Vb, 101011-19-2; VIa, 101011-20-5; VIc, 101011-21-6; CO, 630-08-0; closed-$Fe_3(CO)_8(\mu_3\text{-}PPh)_2[PPh_3]^{-\cdot}$, 101011-22-7; open-$Fe_3(CO)_8(\mu_3\text{-}PPh)_2[PPh_3]^{-\cdot}$, 101011-24-9; open-$Fe_3(CO)_8(\mu_3\text{-}PPh)_2[P(OPh)_3]^{-\cdot}$, 101011-26-1; $P(OMe)_3$, 121-45-9; PEt_3, 554-70-1.

Supplementary Material Available: Tables of complete bond distances, bond angles, anisotropic thermal parameters, and structure factor amplitudes for the tris-phosphite IV (15 pages). Ordering information is given on any current masthead page.

Resonance Raman Spectroscopy of Metallochlorins. 2. Properties of Meso-Substituted Systems

Laura A. Andersson,[†] Thomas M. Loehr,*[†] Chariklia Sotiriou,[‡] Weishih Wu,[‡] and Chi K. Chang[‡]

Contribution from the Department of Chemical, Biological, and Environmental Sciences, Oregon Graduate Center, Beaverton, Oregon 97006-1999, and the Department of Chemistry, Michigan State University, East Lansing, Michigan 48824. *Received September 9, 1985*

Abstract: Nickel(II) and copper(II) complexes of meso-substituted chlorins (dihydroporphyrins) have been examined by FTIR and resonance Raman (RR) spectroscopy to determine whether their vibrational characteristics are in agreement with the observed properties of physiological chlorins (protoporphyrin IX-derived) recently reported by Andersson et al. (*J. Am. Chem. Soc.* **1985**, *107*, 182–191). The first red (647.1-nm) excitation spectra of a metallochlorin are presented, along with an excitation profile. The IR and RR spectra of nickel(II) *meso*-tetramethylchlorin (NiTMC) and copper(II) *meso*-tetraphenylchlorin (CuTPC) are considerably more complex than spectra of the analogous porphyrins. Despite the altered pattern of peripheral substituents in the meso-substituted metallochlorin systems, it is clear that a common set of vibrational properties is applicable to both meso-substituted and physiological metallochlorins: (a) an increase in the total number of RR bands; (b) an increase in the number of polarized RR bands; (c) the notable presence of one or more new polarized "chlorin" bands in the region of the oxidation-state marker; (d) altered polarization properties for B_{1g} and A_{2g} modes; (e) RR-active, split E_u (D_{4h} symmetry) modes; (f) predominance of polarized vibrational modes with both Soret and visible excitation; and (g) nearly identical frequencies in both IR and RR spectra. The observation that metallochlorin vibrational properties can be generalized extends the utility of such parameters to cover a wider variety of metallochlorins than has been studied to date and will aid in the understanding of metallochlorins both as model complexes and in biological systems such as the chlorophylls and/or the chlorin-containing green heme proteins.

Extensive investigations of biological and model metalloporphyrin systems by resonance Raman (RR) spectroscopy have established its utility as a probe of the characteristic molecular properties of these chromophores. This body of work, which has recently been reviewed,[1] includes identification of metalloporphyrin oxidation states and spin states, analysis of the effects of the central metal ion, examination of the influences arising from the type and number of axial ligands, assignment of low-frequency metal–ligand vibrations, assignment of vibrations arising from macrocyclic substituents (e.g., vinyl and formyl modes), and, where appropriate,

* To whom correspondence should be addressed.
† Oregon Graduate Center.
‡ Michigan State University.

(1) Spiro, T. G. In *Iron Porphyrins, Part II*; Lever, A. B. P., Gray, H. B., Eds.; Addison-Wesley: Reading, MA, 1983; Chapter 3.

0002-7863/86/1508-2908$01.50/0

Table I. Assignments of $Ni^{II}TMC$ and $Cu^{II}TPC$ Optical Transitions[a]

	$Q_y(0,0)$	$Q_y(0,1)$	$Q_y(0,2)$	$Q_x(0,0)$	$Q_x(0,1)$	B_y	B_x[c]
$Ni^{II}TMC$	16 225 (616.3)	17 360 (576)	18 700[b] (535)	19 700[b] (508)		23 800 (420.2)	25 250 (396)
$Cu^{II}TPC$	16 225 (616.3)	17 360 (576)	18 250 (542)	19 610 (509)	21 000 (476)	24 150 (414.1)	25 380 (394)

[a] 0,0, 0,1, and 0,2 refer to electronic transitions involving zero, one, and two simultaneous vibrational excitations, respectively; absorption maxima in wavenumbers (nanometers). Samples in CH_2Cl_2 solution. [b] See Figure 6. [c] Alternatively, this may be an η transition.[32]

study of the influences of the protein on the prosthetic group. The vibrational spectroscopic properties of the nonbiological meso-substituted metalloporphyrins have been shown to have substantially altered patterns from those of the "physiological" metalloporphyrins, although many similarities do exist.[2-11]

In contrast, the vibrational properties of partially saturated metalloporphyrins such as chlorins (dihydroporphyrins) are considerably less well defined. Biological reduced heme systems that have been studied by RR spectroscopy include chlorophylls,[12] bacterial cytochromes *d* and d_1,[13-16] leukocyte myeloperoxidase,[17,18] bovine spleen green heme protein,[18] and sulfmyoglobin.[19] Reports of RR spectra of model metallochlorins include that of Ozaki et al.[20] and the recent analyses from our laboratory.[21]

Our initial goals were to define general RR spectroscopic parameters by which one may distinguish metallochlorins from metalloporphyrins and by which one could verify the presence of the chlorin macrocycle in a biological system of undefined prosthetic group structure.[19,21] By comparisons of the RR spectra of sulfmyoglobin with myoglobin, of protoporphyrin IX-related iron chlorins with the analogous iron porphyrins, and of previously published data on metallooctaethylchlorins and -porphyrins, we have established a set of criteria unique to the vibrational properties of chlorin-containing proteins and chlorin model complexes.[19,21] However, for such parameters to be more widely applicable, it is necessary to demonstrate that they can be extended to other systems such as meso-substituted metallochlorins. The work presented in this paper addresses this issue.

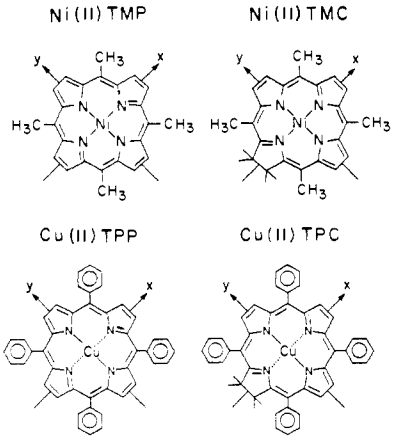

Figure 1. Structures of $Ni^{II}TMP$, $Ni^{II}TMC$, $Cu^{II}TPP$, and $Cu^{II}TPC$.

We have performed a comparative analysis of the FTIR and RR spectroscopic properties of meso-substituted nickel(II) tetramethylchlorin and copper(II) tetraphenylchlorin with their respective porphyrin analogues (Figure 1). The results of this study clearly demonstrate that a generalized set of vibrational parameters exists which is applicable to metallochlorins, regardless of their pattern of substitution.

Experimental Section

Nickel(II) *meso*-tetramethylporphyrin (NiTMP) and nickel(II) *meso*-tetramethylchlorin (NiTMC) were the generous gift of Prof. K. M. Kadish;[22] nickel(II) *meso*-tetramethylchlorin-d_{12} was synthesized according to Ulman et al.[23] using acetaldehyde-d_4 (99+% deuteration; Aldrich) and pyrrole. Copper(II) *meso*-tetraphenylporphyrin (CuTPP) was purchased from Aldrich. Tetraphenylchlorin (TPC) and TPC-d_{20} were synthesized by diimide reduction of TPP and TPP-d_{20}, respectively, according to Whitlock et al.[24] Copper insertion was accomplished by heating a $CHCl_3$ solution of the chlorin with copper(II) acetate in CH_3OH. TPP-d_{20} was synthesized by the previously reported methods of Dolphin and co-workers.[25] IR spectra were obtained from KBr pellets or in CS_2 solution on a Perkin-Elmer Model 1800 FTIR instrument. Raman samples (~0.5 to 1.0 mg/mL) were prepared anaerobically in freshly distilled CH_2Cl_2, benzene, or CCl_4. Samples were transferred via Hamilton gas-tight syringes to N_2-purged standard melting point capillaries, frozen in liquid nitrogen, and the capillaries flame-sealed. Absorption spectra of the samples were recorded on a Perkin-Elmer Lambda 9 spectrophotometer, both before and after the RR experiments, and found to be unchanged as a result of laser irradiation. Resonance Raman spectra of the complexes were obtained with 457.9-, 488.0-, 514.5-, 568.2-, and 647.1-nm excitations (Spectra-Physics 164-05 Ar and 164-01 Kr ion lasers) from samples maintained at ~−10 to 2 °C, using either backscattering from a sample Dewar[26] or 90° scattering from a Varian E4540 variable-temperature accessory. The computer-controlled Raman spectrophotometer and data reduction programs have been reported previously.[27] Depolarization ratios were calculated from peak heights in spectra obtained by rotation of the polarization incident on the sample fixed in the 90° geometry.[28] The excitation profile of NiTMC, using

(2) Mendelsohn, R.; Sunder, S.; Bernstein, H. J. *J. Raman Spectrosc.* **1975**, *3*, 303–312.
(3) Gaughan, R. R.; Shriver, D. F.; Boucher, L. J. *Proc. Natl. Acad. Sci. U.S.A.* **1975**, *72*, 433–436.
(4) Adar, F.; Srivastava, T. S. *Proc. Natl. Acad. Sci. U.S.A.* **1975**, *72*, 4419–4424.
(5) Burke, J. M.; Kincaid, J. R.; Spiro, T. G. *J. Am. Chem. Soc.* **1978**, *100*, 6077–6083.
(6) Burke, J. M.; Kinkaid, J. R.; Peters, S.; Gagne, R. R.; Collman, J. P.; Spiro, T. G. *J. Am. Chem. Soc.* **1978**, *100*, 6083–6088.
(7) Stong, J. D.; Spiro, T. G.; Kubaska, R. J.; Shupack, S. I. *J. Raman Spectrosc.* **1980**, *9*, 312–314.
(8) Chottard, G.; Mansuy, D. *J. Chem. Soc., Chem. Commun.* **1980**, 279–280.
(9) Chottard, G.; Battioni, P.; Battioni, J.-P.; Lange, M.; Mansuy, D. *Inorg. Chem.* **1981**, *20*, 1718–1722.
(10) Aramaki, S.; Hamaguchi, H.; Tasumi, M. *Chem. Phys. Lett.* **1983**, *96*, 555–559.
(11) Stein, P.; Ulman, A.; Spiro, T. G. *J. Phys. Chem.* **1984**, *88*, 369–374.
(12) Lutz, M. In *Advances in Infrared and Raman Spectroscopy*; Clark, R. J. H., Hester, R. E., Eds.; Wiley-Heyden: London, 1984; Vol. 11, pp 211–300.
(13) Poole, R. K.; Baines, B. S.; Hubbard, J. A. M.; Hughes, M. N.; Campbell, N. J. *FEBS Lett.* **1982**, *150*, 147–150.
(14) Cotton, T. M.; Timkovich, R.; Cork, M. S. *FEBS Lett.* **1981**, *133*, 39–41.
(15) Ching, Y.; Ondrias, M. R.; Rousseau, D. L.; Muhoberac, B. B.; Wharton, D. C. *FEBS Lett.* **1982**, *138*, 239–244.
(16) Recent work by C. K. Chang indicates that the chromophore of bacterial heme-d_1 is actually a dioxoisobacteriochlorin, rather than a chlorin (*J. Biol. Chem.* **1985**, *260*, 9520–9522).
(17) Sibbett, S. S.; Hurst, J. K. *Biochemistry* **1984**, *23*, 3007–3013.
(18) Babcock, G. T.; Ingle, R. T.; Oertling, W. A.; Davis, J. S.; Averill, B. A.; Hulse, C. L.; Stufkens, D. J.; Bolscher, B. G. J. M.; Wever, R. *Biochim. Biophys. Acta* **1985**, *828*, 58–66.
(19) Andersson, L. A.; Loehr, T. M.; Lim, A. R.; Mauk, A. G. *J. Biol. Chem.* **1984**, *259*, 15340–15349.
(20) Ozaki, Y.; Kitagawa, T.; Ogoshi, H. *Inorg. Chem.* **1979**, *18*, 1772–1776.
(21) Andersson, L. A.; Loehr, T. M.; Chang, C. K.; Mauk, A. G. *J. Am. Chem. Soc.* **1985**, *107*, 182–191.
(22) Chang, D.; Malinski, T.; Ulman, A.; Kadish, K. M. *Inorg. Chem.* **1984**, *23*, 817–824.
(23) Ulman, A.; Fisher, D.; Ibers, J. A. *J. Heterocycl. Chem.* **1982**, *19*, 409–413.
(24) Whitlock, H. W.; Hanauer, R.; Oester, M. Y.; Bower, B. K. *J. Am. Chem. Soc.* **1969**, *91*, 7485–7489.
(25) Fajer, J.; Borg, D. C.; Forman, A.; Felton, R. H.; Vegh, L.; Dolphin, D. *Ann. N. Y. Acad. Sci.* **1973**, *206*, 349–364.
(26) Sjöberg, B.-M.; Loehr, T. M.; Sanders-Loehr, J. *Biochemistry* **1982**, *21*, 96–102.
(27) Loehr, T. M.; Keyes, W. E.; Pincus, P. A. *Anal. Biochem.* **1979**, *96*, 456–463.

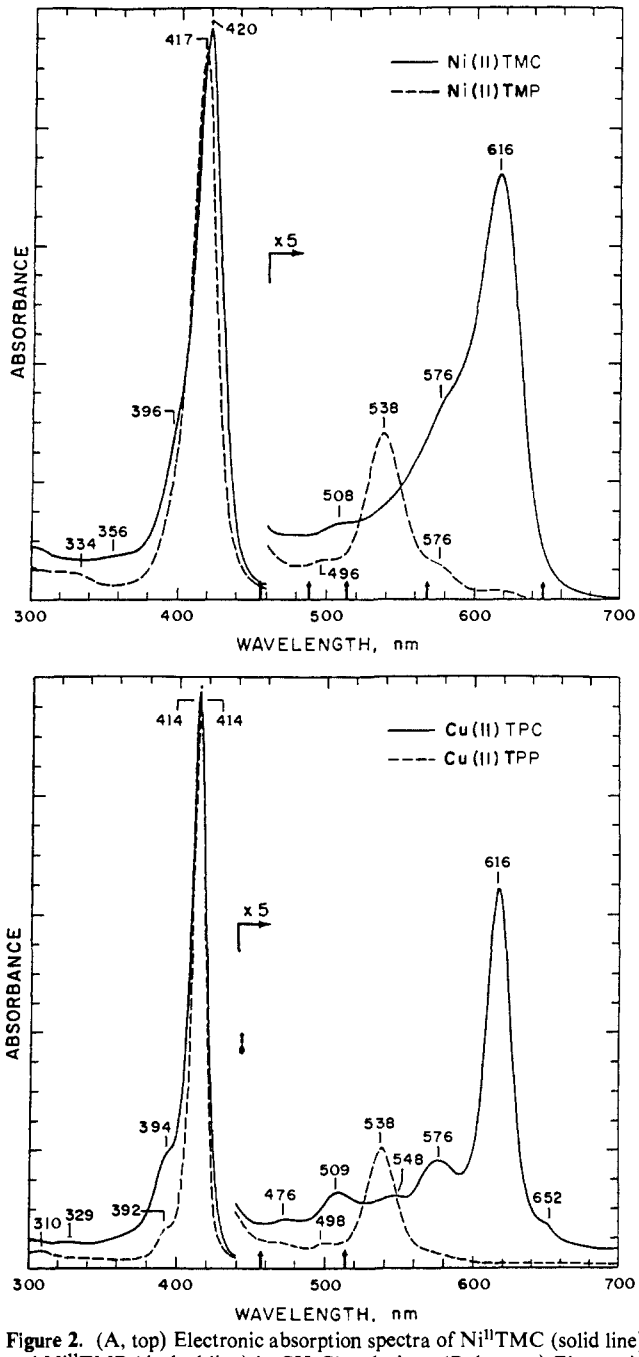

Figure 2. (A, top) Electronic absorption spectra of $Ni^{II}TMC$ (solid line) and $Ni^{II}TMP$ (dashed line) in CH_2Cl_2 solution. (B, bottom) Electronic absorption spectra of $Cu^{II}TPC$ (solid line) and $Cu^{II}TPP$ (dashed line) in CH_2Cl_2 solution. Resonance Raman excitation lines are indicated by arrows. Note: The CuTPC feature labeled as 548 nm should be marked 542 nm.

the CH_2Cl_2 solvent band at 1420 cm^{-1} as a standard, was obtained using excitation lines from 454.5 to 647.1 nm, from Ar, Kr, and He/Ne lasers (Spectra-Physics 125).

Results and Discussion

A. Metallochlorin Molecular Symmetry and Electronic Structure. As shown by X-ray crystallography, metallochlorin and metalloporphyrin molecules may have profoundly different structural properties. For example, whereas NiTMP effectively has D_{4h} symmetry, with a center of inversion and an essentially

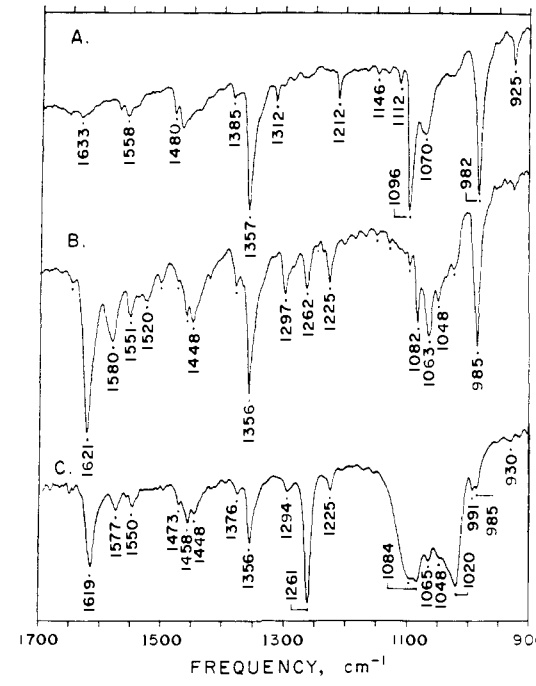

Figure 3. Infrared spectra of (A) $Ni^{II}TMP$, (B) $Ni^{II}TMC$, and (C) $Ni^{II}TMC$-d_{12}, all as KBr pellets.

planar macrocycle, NiTMC is S_4-ruffled, lacks an inversion center, and is consequently "extremely nonplanar".[29] Furthermore, the C_t–C_m distance (central hole) has "decreased considerably" for NiTMC, e.g., 3.380 vs. 3.422 Å for NiTMP.[29] In contrast, Spaulding et al.[30] report that the geometry of $Zn^{II}TPC(py)\cdot C_6H_6$ is not significantly different from that of the analogous porphyrin, with the exception of bond distances in the reduced ring. However, the average C_t–C_m distance for ZnTPC is 3.445 vs. 3.477 Å for ZnTPP,[30] reflecting a decrease in the chlorin central hole of the same order as that reported for NiTMC vs. NiTMP.[29] An analogous S_4 ruffling and reduction in core size for $Fe^{II}OEC$ is reported by Strauss et al.[31]

Metallochlorins exhibit x,y inequivalence with respect to their inner π-conjugation pathways,[21,32] resulting in loss of degeneracy in the two pairs of orbitals which make up the four-orbital model.[32] Of the four transitions which connect the four energy levels, two are strongly allowed and two Soret bands are observed in spectra of many metallochlorins.[21,33] However, where accidental degeneracy has occurred, a single Soret band may result. The lowest energy Q transition is more strongly allowed relative to porphyrin Q bands and produces the intense "chlorin" transition observed at ~600 nm; the other Q transition is almost parity forbidden and therefore relatively weak.[32] Figure 2 presents electronic absorption spectra of NiTMC, CuTPC, and the analogous porphyrin complexes. Absorption bands for the chlorin complexes are assigned in Table I, using the convention of Weiss.[32] $Q_y(0,0)$ and $Q_x(0,0)$ bands are virtually identical for both NiTMC and CuTPC, respectively (Table I). The spectra of NiTMC and CuTPC both have high-energy shoulders near the Soret band which are assigned as the B_x transitions but could alternately be η transitions with a degenerate Soret.[32] The Q_x transitions are clearly evident in the CuTPC spectrum but are not as well resolved in the NiTMC spectrum (Figure 2). However, the NiTMC

(28) Although $\rho < 0.75$ qualifies as polarized, we have used a stricter convention of $\rho < 0.5$ for these data. Depolarized vibrational modes can have $\rho \simeq 0.6$–0.7, with Soret and near-Soret excitation arising from polarization dispersion.[1] Also, since virtually all vibrational modes are Raman-allowed for the chlorins, considerable overlap of polarized and depolarized bands may occur, rendering measurements of depolarization ratios more difficult.

(29) Gallucci, J. C.; Swepston, P. N.; Ibers, J. A. *Acta Crystallogr., Sect. B* **1982**, *B38*, 2134–2139.
(30) Spaulding, L. D.; Andrews, L. C.; Williams, G. J. B. *J. Am. Chem. Soc.* **1977**, *99*, 6918–6923.
(31) (a) Strauss, S. H.; Silver, M. E.; Long, K. M.; Thompson, R. G.; Hudgens, R. A.; Spartalian, K.; Ibers, J. A. *J. Am. Chem. Soc.* **1985**, *107*, 4207–4215. (b) Strauss, S. H.; Silver, M. E.; Ibers, J. A. *J. Am. Chem. Soc.* **1983**, *105*, 4108–4109.
(32) Weiss, C. In *The Porphyrins*; Dolphin, D., Ed.; Academic: New York, 1978; Vol. 3, Chapter 3.
(33) Scheer, H.; Inhoffen, H. H. In *The Porphyrins*; Dolphin, D., Ed.; Academic: New York, 1978; Vol. 2, pp 45–90.

Table II. IR Frequencies for NiTMP and NiTMC[a]

proposed porphyrin assignments[b]	NiTMP	NiTMC	NiTMC-d_{12}	proposed chlorin assignments
		1647		$\nu_{37}(1)$ C_aC_m
ν_{37} E_u C_aC_m	1633[c]			
		1621	1619	$\nu_{37}(2)$ C_aC_m
		1580	1577	$\nu_{38}(1)$ C_bC_b
ν_{38} E_u C_bC_b	1558[d] (1548)[e]			
		1551	1550	$\nu_{38}(2)$ C_bC_b
		1520	?	
		1498	1498	$\nu_{39}(1)$ C_aC_m
ν_{39} E_u C_aC_m	1480[d]			
		1472	1473	$\nu_{39}(2)$ C_aC_m
		1458	1458	
		1448	1448	$\nu_{40}(1)$ C_aC_b
ν_{40} E_u C_aC_b	1439[d] (1438)			
		1420	?	$\nu_{40}(2)$ C_aC_b
	1385[d]			
		1377	1376	ν_{12} C_aN
		1365		$\nu_{41}(1)$ C_aN[g]
ν_{41} E_u C_aN + methyl	1357[c] (1343)	1356	1356	ν_4 C_aN
		1342		$\nu_{41}(2)$ C_aN[g]
			1294	
ν C_mCH_3	1312	1297	1261	ν C_mCH_3
		1262		
		1225	1225	
	1212			
		1202		
ν_{43} E_u C_aN	1146[d] (1154)	1147		$\nu_{43}(1)$ C_aN
		1127		$\nu_{44}(1)$ C_aC_b
ν_{44} E_u C_aC_b	1112[d] (1121)			
	1096 (1092)	1094	1095	$\nu_{44}(2)$ C_aC_b
		1082	1084	$\delta_{as}(1)$ C_bH
ν_{44} E_u δ_{as} C_bH	1070[f]			
		1063	1065	$\delta_{as}(2)$ C_bH
		1048	1048	
		1023	1020	
			991	
ν C_mCH_3	982[d] (979)	985	803	νC_mCH_3
ν_{46} E_u C_aC_m	925[d]	925	930	$\nu_{46}(1)$ C_aC_m

[a] NiTMP IR spectrum obtained as KBr pellet; NiTMC IR obtained both as KBr pellet and in CS_2 solution; NiTMC-d_{12} IR obtained as KBr pellet. [b] Mode numbering system and major contributing coordinates adapted from ref 35. [c] In agreement with calculated frequency for NiOEP, ref 35. [d] In agreement with observed frequency for NiOEP, ref 35. [e] ( ) = frequencies for free-base TMP, ref 2 and 36. [f] In agreement with observed frequency for CuTPP, Table IV. [g] Plus meso-methyl contribution.

transitions can be more readily observed in the spectrum shown in Figure 6. In general, the absorption bandwidths for CuTPC are narrower than those of NiTMC. Absorption spectra of NiTMC[22] and CuTPC[34] have been previously reported, although without assignments.

The effective $C_2(x)$ molecular symmetry of metallochlorins[21] results in both altered IR and Raman spectra since in-plane E_u and out-of-plane A_{2u} IR modes (D_{4h} symmetry) are no longer Raman forbidden, while in-plane A_{1g}, B_{1g}, B_{2g}, and A_{2g} and out-of-plane E_g Raman modes (D_{4h} symmetry) are no longer IR forbidden. Hence, porphyrin E_u and E_g modes become split into chlorin A (polarized) and B (depolarized) components, whereas porphyrin A_{1g} and B_{1g} modes both become chlorin A modes and porphyrin A_{2g}, A_{2u}, and B_{2g} modes become chlorin B modes. The general effect is an increase in the total number of IR and Raman allowed modes, with observation of bands at similar frequencies in both IR and RR spectra, and an increase in the number of polarized Raman modes.

B. Infrared Properties of Nickel(II) *meso*-Tetramethylchlorin and -porphyrin. High-frequency (>900 cm^{-1}) IR spectra of NiTMP and NiTMC are presented in Figure 3. Their frequencies and proposed assignments are listed in Table II. Because NiTMP has an inversion center, the IR- and Raman-allowed vibrational modes are mutually exclusive, and only E_u and A_{2u} modes are expected in the IR, whereas high-frequency Raman features should be predominantly in-plane A_{1g}(p), B_{1g}(dp), A_{2g}(ap), and B_{2g}(dp) modes. Furthermore, the meso pattern of substitution for NiTMP affects the mode composition and contributions, relative to those of nickel(II) octaethylporphyrin (NiOEP). For example, six new vibrational bands are expected for in-plane stretching and bending modes of the meso methyl substituents of NiTMP [ν: A_{1g}, B_{2g}, E_u. δ: B_{1g}, A_{2g}, E_u]. For the in-plane stretching and bending modes of the pyrrole hydrogens, 12 new bands are expected [ν_s: A_{1g}, B_{1g}, E_u. ν_{as}: A_{2g}, B_{2g}, E_u. δ_s: A_{1g}, B_{1g}, E_u. δ_{as}: A_{2g}, B_{2g}, E_u].[11] Of these, the six C_bH stretches should occur $\geq$ 2800 cm^{-1} and are thus not observed in the spectra reported herein. Additional IR bands can also be expected from internal vibrations of the meso-methyl substituents. According to Mason,[36] the methyl group vibrations should be lowered relative to their normal range due to steric hindrance between the methyl substituent and the β-CH groups of the two adjacent pyrrole rings. Bending and stretching modes or contributions attributable to the meso hydrogens or the pyrrole substituents of OEP are not applicable to the TMP spectra. Finally, significant alterations of vibrational couplings are also expected, such as mixing of the C_bH bending coordinates with other high-frequency porphyrin ring modes.[1] However, with these exceptions, the majority of the assignments made by Abe and co-workers[35] should be (loosely) transferable to TMP.

In the NiTMP IR spectrum (Figure 3; Table II), bands at 1633, 1558, 1480, 1439, 1357, 1146, and 1112 cm^{-1} are likely candidates for E_u modes ν_{37}–ν_{44}, respectively; ν_{42} is not observed in NiTMP or NiTMC spectra because it consists of OEP modes not transferable to the meso systems (C_mH bending and C_b substituent stretching).[35] The majority of the proposed E_u IR modes observed for NiTMP are close in frequency to the corresponding NiOEP modes,[35] providing support for our suggested assignments. The IR band at 1312 cm^{-1} (Figure 3) may be the degenerate asymmetric stretching mode of the meso carbons and their methyl substituents, since this band is not observed in IR spectra of NiOEP[35,37] or of CuTPP (see Figure 7). The IR feature at ~1070 cm^{-1} is likely to be the asymmetric bending mode of the pyrrole carbons and their hydrogen substituents. This band also occurs as a strong feature in IR spectra of CuTPP[38] at ~1070 cm^{-1} (Figure 7A and Table IV) but is absent from NiOEP spectra.[35,37] In agreement with the symmetry predictions, infrared frequencies for NiTMP generally do not correlate with the RR frequencies (see below).

The increased complexity of the NiTMC IR spectrum is immediately evident and is attributable to the decrease in effective molecular symmetry and resulting loss of mutual exclusion. Since porphyrin A_{1g}, B_{1g}, A_{2g}, B_{2g}, and E_g modes become IR-active, one can expect not only to observe new IR bands but also altered intensity patterns where vibrational modes of similar frequency and character overlap. The most notable new feature is a strong band at 1621 cm^{-1}; an IR band near this frequency is characteristic of chlorins.[33] The predicted splitting of porphyrin E_u modes is apparent for many of the NiTMC IR features. For example, ν_{37} in the NiTMP IR spectrum occurs at 1633 cm^{-1}, but in the NiTMC IR spectrum, two features are observed at 1647 and 1621 cm^{-1} whose average frequency is 1634 cm^{-1}. Other apparent examples of E_u splitting include ν_{38}, ν_{39}, ν_{40}, ν_{41}, and ν_{44}. In each of these cases, two features are observed in the NiTMC IR spectrum, with an average frequency for the pair which is within 3–7 cm^{-1} of the observed NiTMP frequency.

For most of the NiTMC IR modes, analogous bands occur in the RR spectra (Figures 4 and 5), as expected. For example, ν_{41}

(34) Dorough, G. D.; Huennekens, F. M. *J. Am. Chem. Soc.* **1952**, *74*, 3974–3976.
(35) Abe, M.; Kitagawa, T.; Kyogoku, Y. *J. Chem. Phys.* **1978**, *69*, 4526–4534.
(36) Mason, S. F. *J. Chem. Soc.* **1958**, 976–982.
(37) Choi, S.; Spiro, T. G.; Langry, K. C.; Smith, K. M. *J. Am. Chem. Soc.* **1982**, *104*, 4337–4344.
(38) Alben, J. O.; Choi, S. S.; Adler, A. D.; Caughey, W. S. *Ann. N. Y. Acad. Sci.* **1973**, *206*, 278–295.

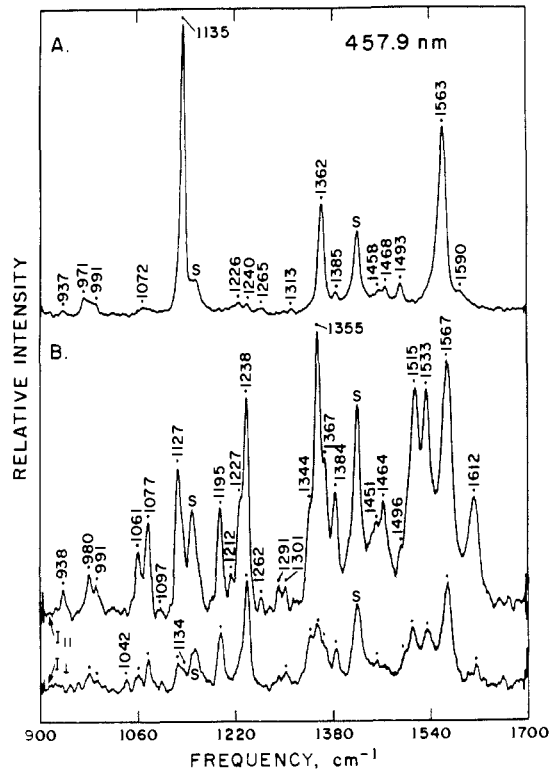

Figure 4. Resonance Raman spectra of $Ni^{II}TMP$ and $Ni^{II}TMC$, 457.9-nm excitation. (A) $Ni^{II}TMP$, ~1 mg/mL in CH_2Cl_2; backscattering geometry. Conditions: laser power, 40 mW at sample Dewar; slit width, 5 cm^{-1}; scanning speed, 2 cm^{-1}/s with repetitive scanning. (B) $Ni^{II}TMC$, ~0.5 mg/mL in CH_2Cl_2; 90° scattering geometry; top $I_\parallel$, bottom $I_\perp$; other conditions as above.

at 1357 cm^{-1} in the NiTMP IR spectrum has apparently split into two bands at 1365 and 1342 cm^{-1} in the NiTMC IR (the latter band is resolved in CS_2 solution IR spectra; data not shown) with a concomitant new pair in the NiTMC RR at 1370 (p) and 1344 (dp) cm^{-1}. The polarization properties of these two bands are in agreement with those predicted for split E_u modes. It is plausible that the band at 1356 cm^{-1} is the IR-active ν_4 in the NiTMC IR spectrum. The 1312-cm^{-1} asymmetric C_mCH_3 stretching mode of NiTMP apparently also splits in the NiTMC spectra, to a new strong band at 1297 cm^{-1} and to a weaker, unresolved band at >1312 cm^{-1}. This hypothesis is supported by the NiTMC-d_{12} spectra, wherein the 1297-cm^{-1} feature is decreased, revealing an underlying band at 1294 cm^{-1}, and the 1261-cm^{-1} feature is increased (Figure 3; Table II). Furthermore, the 1312-cm^{-1} feature of NiTMP, the 1297-cm^{-1} feature of NiTMC, and the 1261-cm^{-1} band of NiTMC-d_{12} are all absent from the CuTPP, CuTPC, and CuTPC-d_{20} spectra (Figure 7; Table IV).

The IR spectrum of NiTMC-d_{12} (deuterated meso methyls) differs from that of NiTMC both in band frequencies and in their relative intensities. The medium-intensity band at ~1262 cm^{-1} in the NiTMC spectrum has become dominant in the NiTMC-d_{12} spectrum (Figure 3) and is likely to be the asymmetric C_mCH_3 mode. The intense peak at ~985 cm^{-1} in both the NiTMP and NiTMC spectra is significantly decreased in the NiTMC-d_{12} spectrum, which has a new strong band at ~803 cm^{-1} (data not shown), indicating involvement of the meso methyl substituents in this vibrational mode. Other changes include an increased intensity for the NiTMC-d_{12} bands at 1458 and 1020 cm^{-1}, as well as a loss of intensity at ~1520, 1065, and 930 cm^{-1}.

C. Resonance Raman Properties of Nickel(II) *meso*-Tetramethylchlorin and -porphyrin. Resonance Raman spectra of NiTMP and NiTMC obtained with near-Soret excitation (457.9 nm) are shown in Figure 4. Spectra of NiTMP, NiTMC, and NiTMC-d_{12} obtained with visible excitation (647.1 nm) at the edge of the "chlorin" band are shown in Figure 5. Frequencies and proposed assignments of these and other RR data are given in Table III. Excitation profiles for selected RR bands of NiTMC

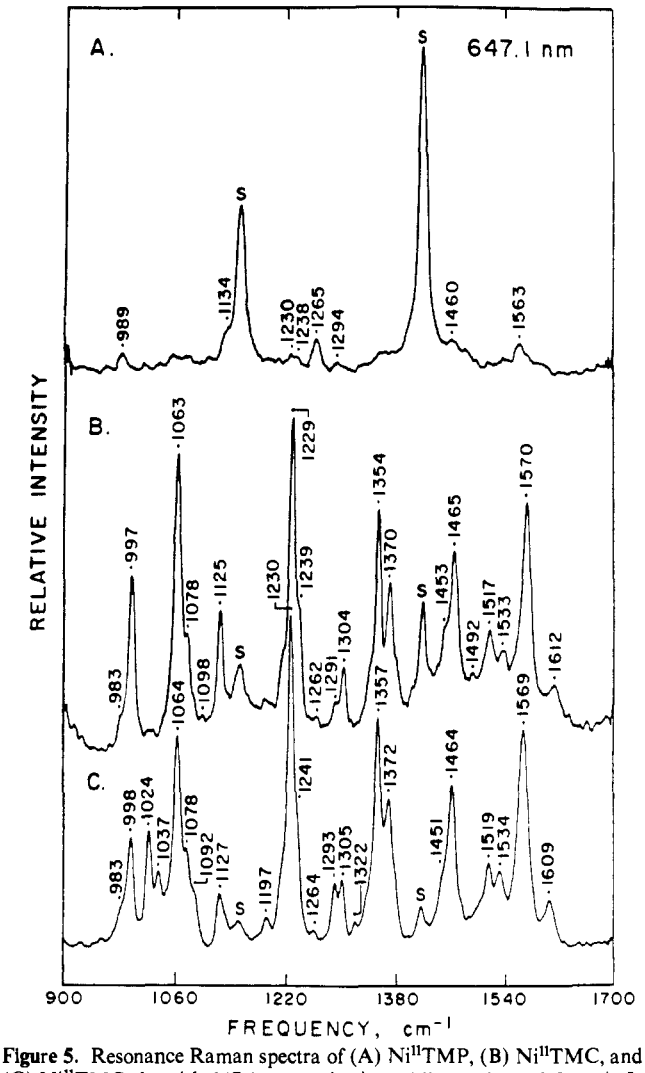

Figure 5. Resonance Raman spectra of (A) $Ni^{II}TMP$, (B) $Ni^{II}TMC$, and (C) $Ni^{II}TMC$-d_{12} with 647.1-nm excitation. All samples ~0.5 mg/mL in CH_2Cl_2, 90° scattering geometry, laser power 120 mW at sample; other conditions as in Figure 4A.

sampling the enhancement by the Q-band manifold are shown in Figure 6.

From our previous RR studies of metallochlorins vs. metalloporphyrins, we noted a general pattern for chlorins that includes the following: (a) an increase in the number of RR bands; (b) an increase in the number of polarized (totally symmetric) RR bands; (c) the presence of one or more new polarized chlorin bands in the region of ν_4, the oxidation-state marker; (d) altered polarization properties for porphyrin B_{1g} and A_{2g} modes; (e) RR-active, split E_u (D_{4h} symmetry) modes; and (f) the predominance of polarized vibrational modes with both Soret and visible excitation.[19,21]

This spectral pattern is clearly displayed by NiTMC. Whereas only three strong, polarized features are observed in the 457.9-nm excitation spectrum of NiTMP, a dozen or more polarized bands occur in the NiTMC spectrum (Figure 4). This contrast in both the total number of bands and the number of polarized bands between the two compounds is maintained for all B and Q band excitation wavelengths. Comparison of the proposed assignments for NiTMP and NiTMC indicates that C_aC_m and C_mCH_3 modes exhibit frequency alterations larger than those of C_bC_b or C_bH modes. Such a pattern could correlate with the altered aromaticity of the chlorins, particularly in the region of the meso carbons.[33]

The NiTMP spectrum has a single strong polarized feature at 1362 cm^{-1}, which we assign to the ν_4 stretching mode of the four equivalent sets of C_a–N bonds having average bond lengths of 1.384 Å.[29] In the NiTMC spectra there are four bands in the same region, at 1384 (p), 1367 (p), 1355 (p), and 1344 (dp) cm^{-1}. The presence of four bands with the indicated polarization

Table III. Resonance Raman Frequencies (cm^{-1}) of Nickel(II) Tetramethylporphyrin and Nickel(II) Tetramethylchlorins[a]

proposed porphyrin assignments[b]	Ni^{II}TMP	Ni^{II}TMC	Ni^{II}TMC-d_{12}[c]	proposed chlorin assignments
		1612 p	1609	ν_{10} C_aC_m A
ν_{10} C_aC_m B_{1g}	1590 dp (1586)[d]			
ν_2 C_bC_b A_{1g}	1563 p	1567 p	1569	ν_2 C_bC_b A
	1550 dp (1543)			
ν_{11} C_bC_b B_{1g}	1532 dp	1533 p	1534	ν_{11} C_bC_b A
		1516 p	1519	
		1510		
		1496 dp		
	1493 dp[e] (1483)			
ν_3 C_aC_m A_{1g}	1468 p[e] (1466)	1465 p	1464	
	1458 dp (1409)	1452 dp	1451	
ν_{12} C_aN B_{1g}	1385 ?	1384 p		ν_{12} C_aN A
		1370 p	1372	ν_{41a} C_aN A
ν_4 C_aN A_{1g}	1362 p	1355 p	1357	ν_4 C_aN A
		1344 dp		ν_{41b} C_aN B
			1322	
	1313 (1310)			
		1303	1305	
	1296	1291 dp	1293	
	1265 dp	1262 dp	1264	
	1239 ap	1239 dp	1241	δ C_bH B
	1226 dp (1224)	1228 p	1230	δ C_bH A
		1212 p		
		1195 dp	1197	
ν C_mCH_3	1135 p	1126 p	1024	ν C_mCH_3 A
			1127	
		1097	1092	
		1078 dp	1078	δ_{as} C_bH B
		1062 p	1064	δ_{as} C_bH A
		1042	1037	
	991 p (991)	997 p	998	
		991 p		
		980	983	
	971 p			
	937	938 p		

[a] Reported frequencies were obtained by excitation at 457.9, 448.0, 514.5, 568.2, and 647.1 nm; $\rho = I_\perp/I_\parallel$, p = polarized, dp = depolarized, ap = anomalously polarized; see ref 28. [b] Adapted from ref 5, 11, and 35. [c] ( ) = Frequencies reported for free-base TMP, ref 2. [d] Reported frequencies were obtained by excitation at 457.9, 514.5, and 647.1 nm. [e] In agreement with data from: Li, X.-Y.; Spiro, T. G., unpublished results.

properties is consistent with $C_2(x)$ symmetry of the chlorin macrocycle in which the porphyrin C_a–N stretching modes ν_4 (A_{1g}), ν_{12} (B_{1g}), and ν_{41} (E_u) become ν_4 (A), ν_{12} (A), and ν_{41a} (A) and ν_{41b} (B), respectively. Furthermore, the observation of multiple bands in this region may reflect the diversity of C_a–N bond lengths determined for the crystal structure of NiTMC, ranging from 1.369 to 1.396 Å.[29] The presence of several polarized bands in the region of ν_4 is one of the most obvious characteristics of metallochlorin RR spectra.

Polarized bands in the NiTMP spectra at ~1563 and 1468 cm^{-1} are assigned as ν_2 and ν_3, respectively. The intense, polarized 1135-cm^{-1} peak is likely to be the symmetric stretching mode of the meso carbons and their methyl substituents. This feature is not observed in RR spectra of metallotetraphenylporphyrins,[2-11] CuTPP (Figure 8), or NiOEP.[34] Resonance Raman spectra of NiTMC-d_{12} (457.9-, 514.5-, 647.1-nm excitation; Figure 5C and Table III) do not appear to be significantly different from normal NiTMC. The unaltered frequency and intensity of the strong bands at ~1230 and 1240 cm^{-1} upon meso methyl deuteration very likely eliminate these bands from consideration as C_mCH_3 modes. However, the NiTMC band at 1127 cm^{-1} is significantly

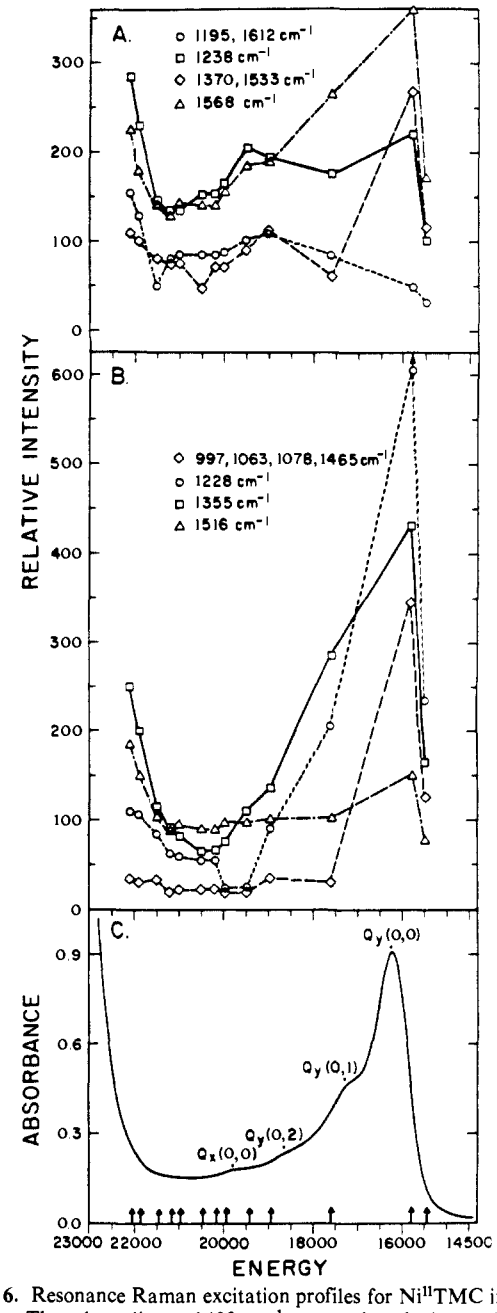

Figure 6. Resonance Raman excitation profiles for Ni^{II}TMC in CH_2Cl_2 solution. The solvent line at 1420 cm^{-1} was used as the internal intensity standard. Relative intensities are expressed as percentages of the 1420-cm^{-1} band height. Bands showing similar behavior are grouped together in a single profile.

altered in the NiTMC-d_{12} spectra, revealing both an underlying feature at ~1124 cm^{-1} and a new band at ~1023 cm^{-1} (Figure 5). The IR spectrum of NiTMC-d_{12} also reveals a new band at 1020 cm^{-1}, in agreement with the Raman data, and serves to establish this frequency as a C_m–CH_3 mode. These observations support our assignment of the 1135-cm^{-1} band in NiTMP. In general, it would appear that vibrational modes of the meso methyl substituents of NiTMP and NiTMC are not resonance-enhanced, although as for the ethyl substituents on the β-pyrrole carbons of NiOEP some coupling with ring modes of the macrocycle does occur. For example, the band at 1612 cm^{-1} in the NiTMC spectra downshifts by 3 cm^{-1} in the NiTMC-d_{12} spectra.

The contrast between NiTMC and NiTMP spectra upon 647.1-nm excitation (Figure 5) is noteworthy. The spectra shown were obtained on identical samples and under identical experimental conditions. Whereas solvent bands dominate over porphyrin modes for the NiTMP spectrum, for which the excitation wavelength lies outside of the Q absorption band, the reverse is true for the NiTMC spectrum. This is the first RR spectrum to

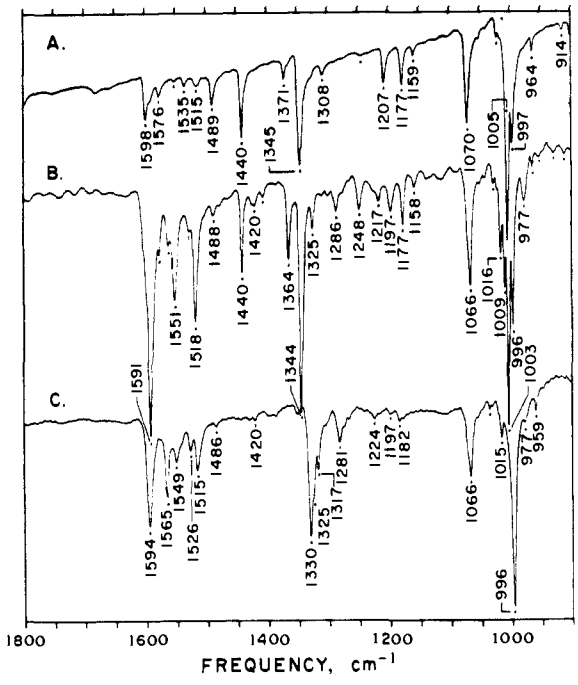

Figure 7. Infrared spectra of (A) $Cu^{II}TPP$, (B) $Cu^{II}TPC$, and (C) $Cu^{II}TPC$-d_{20}, all as KBr pellets.

be presented of a metallochlorin excited within the chlorin absorption band. Previous investigations may have been hampered by fluorescence from traces of free-base chlorin contaminants,[20,21] by dilute samples,[17] or by the inherent fluorescent properties of species such as the chlorophylls.[12]

Comparison of the NiTMC RR spectra obtained with near-Soret and near-Q_y excitation also reveals a contrast in the patterns of enhancement (Figures 4B and 5B). For example, bands at 1077 and 1238 cm^{-1} dominate over adjacent bands at 1061 and 1227 cm^{-1} with 457.9-nm excitation, whereas the reverse is observed upon 647.1-nm excitation. In addition, bands at ~997 and 1304 cm^{-1}, which were fairly weak with 457.9-nm excitation, are more strongly enhanced with red excitation, whereas of the four strong bands in the 1500–1620-cm^{-1} region only the ~1570-cm^{-1} band remains intense with red excitation.

The variation in intensity of selected RR lines of NiTMC as a function of excitation wavelength is shown in Figure 6. These are the first RR excitation profiles to be reported for a metallochlorin system to our knowledge. Three distinct patterns are observed for the NiTMC bands: first, bands which exhibit very strong Q_y resonance enhancement but only minimal Q_x excitation (e.g., 997, 1063, 1078, 1228, and 1465 cm^{-1}); second, bands having minimal enhancement by the Q_y transitions but some Q_x enhancement (e.g., 1195, 1516, and 1612 cm^{-1}); and third, bands showing resonance enhancement by both the Q_x and Q_y transitions (e.g., 1238, 1355, 1370, 1533, and 1568 cm^{-1}). Very strong resonance enhancement was observed with 632.8-nm excitation to the extent that the 1420-cm^{-1} solvent band had essentially vanished. Thus the ~1238-cm^{-1} band, which is an unresolved shoulder at this excitation wavelength, may well belong in the second category having minimal Q_y enhancement. Enhancement profiles for hemeproteins and model compounds using visible light excitation fall into two groups: those having constant maxima (α-band excitation) and those exhibiting shifted maxima (β-band excitation).[1,39] No such displacements are apparent in the present data above the vibronically excited $Q_y(0,1)$ and $Q_x(0,1)$ components. However, the presence of four closely spaced electronic transitions which are dominated by the intense $Q_y(0,0)$ chlorin band would render such resolution in the excitation profiles more difficult to detect experimentally. The preponderance of Raman lines of the NiTMC spectra appear to be efficiently enhanced via coupling to the Q_y transition(s) which, of course, is both the more intense transition and represents the longer π-conjugation pathway through the plane of the molecule.

(39) Felton, R. H.; Yu, N.-T. In *The Porphyrins*; Dolphin, D., Ed.; Academic: New York, 1978; Vol. 3, Chapter 8.

Table IV. Infrared and Resonance Raman Frequencies (cm^{-1}) of Copper(II) Tetraphenylporphyrin and Copper(II) Tetraphenylchlorins[a]

$Cu^{II}TPP$		$Cu^{II}TPC$		$Cu^{II}TPC$-d_{20}	
IR	RR	IR	RR	IR	RR
			1620 dp		
					1610
1598 m	1596 p		1601	1594 s	1597
		1591 vs	1593 p	1565 m	1564
	1581				
1576 w		1577 w, sh	1572 dp		
	1558 p	1563 w, sh			
		1551 s	1551 p	1549 w	1553
1535 w					1537
	1530	1528 w	1528 p	1526 w	1520
1515 w	1518	1518 s	1517 p	1515 m	1512
	1498				1495
1489 m		1488 w	1488 p	1486 w	1490
			1462 p		1466
			1450		1450
1440 s		1440 s	1437 p		1439
		1420 w		1420 vw	
		1407 w			
	1392		1394 p		
					1380
1371 m					
	1361 p	1364 s	1359 p		
				1350 w	1354
1345 s		1344 vs			
	1338		1339 p		1334
				1330 s	
		1325 m	1324	1325 m, sh	1327
1308 w			1313 dp	1317 m	1315
			1300 p		1300
		1286 m	1283 dp	1281 m	1283
	1278	1275 w	1271 p	1275 w	
			1261		1267
		1248 m			
			1241 p		1183
	1235 p		1232 p	1224 w	1228
		1217 w	1213		
1207 m					
		1197 m	1190	1197 vw	
1177 m	1182	1177 m	1180	1182 w	
			1170		1173
1159 w		1158 w			
	1138				1134
	1078		1075 p		1074
1070 s					
		1066 s	1060 p	1066 m	1059
	1050				
	1031 p		1032 p		1035
		1016 m	1017 p	1015 w	1019
		1009 s			
1005 vs	1003	1003 vs	1005 p		1006
997 s	993 p	996 s	993 dp	996 vs	996
		977 m	974	977 w, sh	
964 w		964 w		959 w	969
					954
		928 w			
914 w		911 w			

[a] Reported RR frequencies were obtained by excitation at 457.9 and 514.5 nm; $\rho = I_\perp/I_\parallel$, p = polarized, dp = depolarized; see ref 28.

D. IR Properties of Copper(II) *meso*-Tetraphenylchlorin. High-frequency IR spectra of CuTPP, CuTPC, and CuTPC-d_{20} are presented in Figure 7; the IR frequencies are presented in Table IV. Many of the CuTPP IR bands were previously tabulated by Mason.[36] For CuTPP, IR bands at 1598, 1345, and 1005 cm^{-1} are all sensitive to meso phenyl deuterium substitution,[38] thus indicating phenyl mode contributions. Little correlation occurs between the CuTPP IR and RR bands, as expected for D_{4h} effective symmetry. IR spectra of free-base TPC have been reported by Alben et al.,[38] who suggested a decreased basicity for

the nitrogen of the TPC reduced ring resulting from the strong electron withdrawal by the saturated double bond.

For CuTPC, the IR- and Raman-allowed vibrational modes are no longer mutually exclusive. Furthermore, the mode compositions and contributions differ from those of β-pyrrole-substituted porphyrins such as M–OEP, with predicted new features arising for the bending and stretching modes of the meso phenyl substituents and for bending and stretching modes of the pyrrole hydrogens, as well as spectral changes resulting from the loss of band contributions attributable to the meso hydrogens or pyrrole substituents of M–OEP.

The complexity of the CuTPC IR spectra is immediately evident and is attributable to the decrease in symmetry as discussed by Alben et al.[38] for free-base TPC. The CuTPC spectrum has new bands at 1551, 1518, 1325, 1286, 1248, 1217, 1197, 1016, 1009, and 977 cm^{-1}. Many of these bands are also present in the CuTPC RR spectra. The altered band pattern in the 900–1100-cm^{-1} region for CuTPC is particularly noteworthy. Alterations in intensity are also evident, such as for the ~1591-cm^{-1} feature of CuTPC. This band is likely to be composed of both the ~1598-cm^{-1} phenyl mode and the characteristic high-frequency IR chlorin mode,[33] since CuTPC-d_{20} has a residual ~1594-cm^{-1} feature, but deuterated CuTPP complexes lose the ~1598-cm^{-1} band.[38] The feature at ~1070 cm^{-1} in the CuTPP, CuTPC, and CuTPC-d_{20} spectra is assigned as a pyrrole–hydrogen bending mode (Table IV), in agreement both with the absence of a shift upon phenyl deuteration and with the observation of an analogous feature at ~1070 cm^{-1} in the IR spectra of NiTMP, NiTMC, and NiTMC-d_{12}. Such an assignment was previously suggested for an IR band at ~1060 cm^{-1} in M–TPP spectra.[38]

Comparison of the CuTPC-d_{20} spectrum and that of CuTPC reveals a number of phenyl-sensitive shifts. For example, the CuTPC-d_{20} spectrum has new features at 1565, 1330, 1317, 1224, 818, 812, 650, 540, and 478 cm^{-1} (not all data shown), while bands at ~1591, 1551, 1518, 1440, 1364, 1344, 1248, 1177, 1016, 1009, 1003, 996, 977, 742, 720, 696, and 680 cm^{-1} (not all shown) in the CuTPC spectrum disappear or exhibit altered intensity. Deuterium sensitivity for CuTPC bands at ~1591, 1344, and 1003 cm^{-1} parallels that observed for CuTPP,[38] suggesting that the meso substituent interactions observed for CuTPP are retained in CuTPC. Furthermore, the IR spectrum of CuTPC-d_{20} has bands at 2290 and 2268 cm^{-1}, in good agreement with IR features of deuteriobenzene at 2292 and 2287 cm^{-1}.[40]

E. Resonance Raman Properties of Copper(II) *meso*-Tetraphenylchlorin. Resonance Raman spectra of CuTPP and CuTPC are shown in Figure 8; the RR frequencies are shown in Table IV. The CuTPP spectra are generally in good agreement with those previously reported.[7,10] Resonance Raman mode assignments for M–TPP have been established by Spiro and co-workers;[5-7,11] additional studies have been presented by Chottard et al.[8,9] and by Schick and Bocian.[41]

The spectra of CuTPP are relatively simple. The two polarized bands at 1557 and 1361 cm^{-1} are assigned to the porphyrin skeletal modes ν_2 and ν_4, respectively, while the polarized bands at 1596, 1235, 1030, and 994 cm^{-1} are assigned as phenyl modes A, C, E, and F, by analogy with the data on $(FeTPP)_2O$ reported by Stein et al.[11]

As was observed for NiTMC, the RR properties of CuTPC fit the predicted spectral properties of metallochlorins. Thus, the 514.5-nm excitation spectrum of CuTPP has few strong bands, whereas the CuTPC spectrum has many such features. CuTPC RR bands at 1551 and 1360 cm^{-1} are assigned as ν_2 and ν_4, respectively; the broad polarized bands at 1595, 1240, 1031, and 1003 cm^{-1} are likely to consist, at least in part, of phenyl modes based on their sensitivity to phenyl deuteration (see below). The CuTPC spectrum also has two strong bands in the region of the oxidation-state marker (ν_4) at 1360 and 1341 cm^{-1}, whereas for

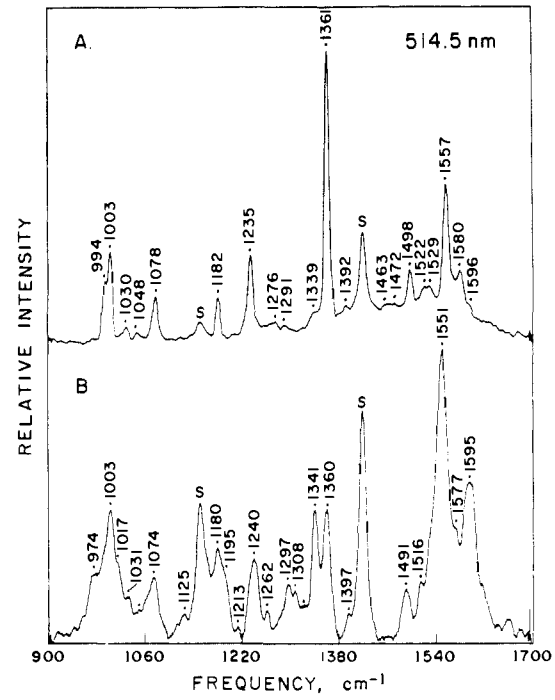

Figure 8. Resonance Raman spectra of $Cu^{II}TPP$ and $Cu^{II}TPC$, 514.5-nm excitation. (A) $Cu^{II}TPP$, ~1.0 mg/mL, backscattering geometry; laser power 90 mW at sample; other conditions as in Figure 4A. (B) $Cu^{II}TPC$, ~1.0 mg/mL, backscattering geometry, other conditions as in Figure 4A.

CuTPP we observe only the feature at 1361 cm^{-1}. The presence of two or more strong bands in the oxidation-state marker region of metallochlorin RR spectra is apparently unaffected by alterations in the identity of the metal ion or the pattern of macrocycle substituents.

Comparision of the spectra of CuTPP and CuTPC reveals both an apparent doubling of most of the CuTPP spectral features and an alteration in the patterns of intensity. For example, the CuTPC bands at ~1595, 1240, 1180, 1074, and 1003 cm^{-1} are considerably broadened, while features at 1595, 1551, and 1360 cm^{-1} have altered in apparent intensity with respect to their CuTPP counterparts. As in the CuTPC IR spectrum, changes in the 900–1100-cm^{-1} region are noteworthy because of an apparently large increase in the total number of bands.

The isotopic shifts observed for CuTPC-d_{20} (Table IV) are in good agreement with those previously reported for $(FeTPP\text{-}d_{20})_2O$.[5,11] For example, CuTPC bands at ~1595 and 1241 cm^{-1} downshift by 29 and 58 cm^{-1}, as compared with shifts of 32 and 50 cm^{-1}, respectively, for FeTPP.[5,11] Furthermore, the intensity of CuTPC bands at 1031 and 1003 cm^{-1} is significantly decreased in the CuTPC-d_{20} spectra, as expected for these phenyl-sensitive modes.[11] The appearance of phenyl modes in the TPP RR spectrum has been attributed to an interaction between the phenyl and porphyrin excited-state π systems.[5] The analogous phenyl dependency evident in the TPC data suggests that such an interaction is preserved upon reduction to the dihydroporphyrin. Furthermore, these data indicate that most of the spectral alterations observed for CuTPC arise as a consequence of the decrease in effective molecular symmetry.

For meso-substituted metalloporphyrins, Stong et al.[7] demonstrated an inverse linear correlation with the core size (C_t–N) and the frequencies of three Raman bands at ~1460 (p), 1540 (ap), and 1570 (p) cm^{-1}. Given that the central holes of CuTPC, NiTMC, and other chlorins are contracted relative to those of the analogous porphyrins,[29-31] one might expect to observe frequency increases for the core-size bands. For both CuTPC and NiTMC, no obvious or direct frequency correlations are apparent in the 1450–1580-cm^{-1} region vis-à-vis the respective porphyrin RR bands. Thus, it would appear either that metalloporphyrin core-size plots are not generally applicable to metallochlorins or that the ruffled structure of the chlorins is responsible for the deviations observed. Clearly, additional study is required in order

(40) Shimanouchi, T. *Tables of Molecular Vibrational Frequencies, Consolidated Volume I*; National Bureau of Standards: Washington, DC, 1972.

(41) Schick, G. A.; Bocian, D. F. *J. Am. Chem. Soc.* **1983**, *105*, 1830–1838.

to define such correlations between chlorin structure and their vibrational properties.

The findings reported here support our hypothesis and previous observations that vibrational spectroscopy, and especially resonance Raman spectroscopy, can be diagnostic for the chlorin macrocycle.[19,21] The spectral criteria that distinguish chlorins from porphyrins appear to hold not only for a large variety of ring substitution patterns and different central metal ions but also when metallochlorins occur as prosthetic groups in metalloproteins. Extension of this work to the analysis of the vibrational properties of bacteriochlorins and isobacteriochlorins (tetrahydroporphyrins) is in progress. These techniques should make it possible to characterize systems that are not amenable to prosthetic group extraction.

Acknowledgment. This research was supported by the National Institutes of Health (GM 34468 to T.M.L. and C.K.C.). We thank Prof. K. M. Kadish for his generous gifts of the NiTMP and NiTMC complexes. We also thank Linda Schmidlin for technical assistance.

Registry No. Cu^{II}TPP, 14172-91-9; Cu^{II}TPC, 52064-15-0; Ni^{II}TMC, 75758-44-0; Ni^{II}TMP, 67067-51-0.

Redox Properties of Metalloporphyrin Dimers

James P. Collman,* Jacques W. Prodolliet,† and Charles R. Leidner

Contribution from the Department of Chemistry, Stanford University, Stanford, California 94305. *Received October 7, 1985*

Abstract: Cyclic and rotated disk voltammetry of two metalloporphyrin dimers, $[Ru(OEP)]_2$ and $[Os(OEP)]_2$, exhibit four oxidations and two reductions for each compound which are all chemically and electrochemically reversible on the voltammetric time scale. Comparison of the formal potentials of the six couples suggests that the first two oxidations are metal-centered redox processes; the remaining four couples are likely to be ligand centered. Controlled chemical oxidations using ferricinium hexafluorophosphate, silver tetrafluoroborate, and tris(4-bromophenyl)ammonium hexachloroantimonate cleanly generate the monocations $[M(OEP)]_2^+$ and the dications $[M(OEP)]_2^{2+}$. NMR, ESR, and electronic spectroscopy of these dimeric, cationic products support the assignment of the two oxidations as metal centered. These oxidations permit the preparation of the two series of metalloporphyrin dimers: paramagnetic $[M(OEP)]_2$ with bond order = 2, paramagnetic $[M(OEP)]_2^+$ with bond order = 2.5, and diamagnetic $[M(OEP)]_2^{2+}$ with bond order = 3.

We have recently developed a new class of binuclear metal complexes M_2L_8 where two metalloporphyrins are joined by a multiple metal–metal bond.[1-3] These dimers were analyzed in terms of a simple molecular orbital diagram (Figure 1), proposed by Cotton[4,5] for quadruply bonded systems This scheme accounts for the ground-state geometry, spin state, and bond order of these dimers solely on the basis of the total number of valence d electrons. The rigid nature of the porphyrin macrocycle, which requires a planar or nearly planar geometry about each metal center, allows the variation of the metal–metal bond orders in these complexes without the interference of bridging ligands, permitting a systematic study of the resulting structural, spectroscopic, and chemical characteristics over the entire bond order range.

Variation of the metal–metal bond orders can be achieved by three different methods: (i) Coupling of two metalloporphyrin monomers containing the same metal in the same oxidation state, M(II), affords the neutral homodimers. Singly (M = Rh,[6,7] Ir[8]), doubly (M = Ru,[1] Os[2]), and quadruply (M = Mo,[2] W[3]) bonded homodimers have been prepared by this technique, but the triply bonded Tc and Re analogues are still unknown. So far only the ruthenium homodimer $[Ru(OEP)]_2$ has been structurally characterized.[9] Furthermore, we were able to measure the rotational barrier of the Mo–Mo quadruple bond in meso-subsituted molybdenum(II) dimers.[10] (ii) Coupling of two metalloporphyrin monomers containing different metals in the same oxidation state should yield neutral heterodimers. This method was used to prepare the only known example of a porphyrin heterodimer containing two transition metals,[11] (OEP)Ru=Os(OEP). This compound, which was observed by ^{1}H NMR, has not been isolated.[2] (iii) Oxidation or reduction of either homo- or heterodimers is a potentially attractive way of preparing ionic dimers with altered metal–metal bond order. This procedure, which has never been used for metalloporphyrin dimers, is the subject of the present paper.

Herein we report the electrochemical and chemical investigation of the redox properties of $[Ru(OEP)]_2$ and $[Os(OEP)]_2$.

Results and Discussion

Electrochemistry of $[Ru(OEP)]_2$ and $[Os(OEP)]_2$. Considerable effort has been made during the last 20 years to understand the redox behavior of metalloporphyrin monomers.[12] It is now recognized that oxidation (or reduction) can occur either at the porphyrin macrocycle, to generatre an organic π cation (or π anion) radical, or at the metal center itself to induce oxidation state changes.[12] However, fewer electrochemical studies on metal–metal bonded complexes have been reported.[13-16] This

† Present address: Institut de Chimie Minerale et Analytique, 3 place du Chateau, CH-1005 Lausanne, Switzerland.

(1) Collman, J. P.; Barnes, C. E.; Collins, T. J.; Brothers, P. J. *J. Am. Chem. Soc.* **1981**, *103*, 7030.
(2) Collman, J. P.; Barnes, C. E.; Woo, L. K. *Proc. Natl. Acad. Sci. U.S.A.* **1983**, *80*, 7684.
(3) Collman, J. P.; Woo, L. K., unpublished results.
(4) Cotton, F. A.; Curtis, N. F.; Harris, C. B.; Johnson, B. F. G.; Lippard, S. J.; Mague, J. T.; Robinson, W. R.; Wood, J. S. *Science (Washington, D.C.)* **1964**, *145*, 1305.
(5) Cotton, F. A. *Inorg. Chem.* **1965**, *4*, 334.
(6) Ogoshi, H.; Setsune, J.; Yoshida, Z. *J. Am. Chem. Soc.* **1977**, *99*, 3869.
(7) Wayland, B. B.; Newman, A. R. *Inorg. Chem.* **1981**, *20*, 3093.
(8) Collman, J. P.; Leidner, C. R.; Garner, J. M.; Johnson, K., unpublished results.
(9) Collman, J. P.; Barnes, C. E.; Sweptson, P. N.; Ibers, J. A. *J. Am. Chem. Soc.* **1984**, *106*, 3500.
(10) Collman, J. P.; Woo, L. K. *Proc. Natl. Acad. Sci. U.S.A.* **1984**, *81*, 2592.
(11) The preparation of a heterometallic porphyrin dimer containing a transition metal and a main group element, (OEP)Rh–In(OEP), has recently been reported by Jones and Wayland (Jones, N. L.; Wayland, B. B. *Abstracts of Papers*, 189th ACS National Meeting of the American Chemical Socety; Miami Beach, FL; American Chemical Society: Washington, DC 1985; Abstract 56).
(12) Davis, D. G. In *The Porphyrins*; Dolphin, D.; Ed.; Academic Press: New York, 1978; Vol. V, p 127.

0002-7863/86/1508-2916$01.50/0